

This is a repository copy of *Modelling Framework and Assistive Device for Peripheral Intravenous Injections*.

White Rose Research Online URL for this paper:

<https://eprints.whiterose.ac.uk/id/eprint/95667/>

Version: Published Version

Article:

Kam, Kin F., Robinson, Martin Paul orcid.org/0000-0003-1767-5541, Gilbert, Mathew Alan et al. (1 more author) (2016) *Modelling Framework and Assistive Device for Peripheral Intravenous Injections*. Open Engineering.

<https://doi.org/10.1515/eng-2016-0005>

Reuse

Items deposited in White Rose Research Online are protected by copyright, with all rights reserved unless indicated otherwise. They may be downloaded and/or printed for private study, or other acts as permitted by national copyright laws. The publisher or other rights holders may allow further reproduction and re-use of the full text version. This is indicated by the licence information on the White Rose Research Online record for the item.

Takedown

If you consider content in White Rose Research Online to be in breach of UK law, please notify us by emailing eprints@whiterose.ac.uk including the URL of the record and the reason for the withdrawal request.

Research Article

Open Access

Kin F. Kam, Martin P. Robinson, Mathew A. Gilbert, and Adar Pelah*

Modelling Framework and Assistive Device for Peripheral Intravenous Injections

DOI 10.1515/eng-2016-0005

Received Aug 06, 2015; accepted Feb 03, 2016

Abstract: Intravenous access for blood sampling or drug administration that requires peripheral venepuncture is perhaps the most common invasive procedure practiced in hospitals, clinics and general practice surgeries. We describe an idealised mathematical framework for modelling the dynamics of the peripheral venepuncture process. Basic assumptions of the model are confirmed through motion analysis of needle trajectories during venepuncture, taken from video recordings of a skilled practitioner injecting into a practice kit. The framework is also applied to the design and construction of a proposed device for accurate needle guidance during venepuncture administration, assessed as consistent and repeatable in application and does not lead to over puncture. The study provides insights into the ubiquitous peripheral venepuncture process and may contribute to applications in training and in the design of new devices, including for use in robotic automation.

Keywords: Needle insertion; Venepuncture; Venous cannulation; peripheral intravenous injection aid; medical device design process; human factors in medical devices; medical robotics

1 Introduction

Peripheral venepuncture (VP) and venous cannulation (VC) are common procedures for medicinal infusion or

blood sampling, with an estimated 3.5 million being performed worldwide each day [1]. These procedures are often unpleasant and require skill and dexterity, delivered confidently in a smooth VP action on a steady site. Failed attempts in venous access via these procedures are unfortunately common, due mostly to difficulty in seeing [2] or accessing the target vein [3], or as a result of inexperience or nervous phlebotomy practitioner. De Boer *et al.* [1] estimate that there are difficulties with as many as one in twenty procedures. A successful VP process (*i.e.* putting the needle or cannula through the skin and accurately into the vein to the right depth, with minimal damage to the venous and surrounding tissues) requires accuracy, skill, confidence, calmness and a steady hand with minimal tension. This combination of requirements coincides with the anticipated inflicting of pain and discomfort on the patient, and the associated anxiety by the practitioner of misplacing the needle often becomes a barrier to a successful VP. It is therefore imperative that practitioners (*e.g.* nurses, doctors, phlebotomists and even some patients) are well trained and understand the varied aspects of VP procedures. In addition, practitioners may derive benefit from the VP process being made easier via an assistive technology, method or device.

There are two methods of carrying out peripheral VP, described as direct and indirect [12]. The direct method is where the needle or cannula enters the skin and immediately enters the vein. This method has the advantage of fewer steps, and for some is easier to learn and perform. There is however anxiety associated with overshooting, that is exiting the vein at its distal membrane, especially with small veins. The alternative, indirect, method involves the needle first entering the skin, often at a less direct or steep angle, then once the vein is relocated or sensed, the practitioner initiates advancing the needle into the vein. The advantage of this approach is that it has a gentler entry, and may be more useful when the vein is less visible or the initial entry has slightly missed the vein. The disadvantages of the indirect method are the requirement for comparatively greater skill and confidence by the practitioner and the potential for greater damage to the skin and vein resulting from the initial shallower entry. The pa-

Kin F. Kam: Inclusive Innovations Ltd., Ron Cooke Hub, University of York, Heslington East, York YO10 5GE, UK; Email: iin-vents@gmail.com

Martin P. Robinson: Department of Electronics, University of York, Heslington, York YO10 5DD, UK; Email: martin.robinson@york.ac.uk

Mathew A. Gilbert: Cambridge Consultants, Science Park, Milton Road, Cambridge CB4 0DW, UK

***Corresponding Author: Adar Pelah:** Department of Electronics, University of York, Heslington, York YO10 5DD, UK; Email: adar.pelah@york.ac.uk.

 © 2016 K. F. Kam *et al.*, published by De Gruyter Open.

This work is licensed under the Creative Commons Attribution-NonCommercial-NoDerivs 3.0 License.

per analyses the motion associated with the act of peripheral VP in the direct method, as the indirect method requires consideration of a wide range of additional parameters that are difficult to model, including variations in device, skin and vein properties, and human interaction factors such as biomechanical feedback.

We show how the VP procedure can be modelled mathematically, such that the path taken by the needle can be predicted or prescribed for potential applications to automation or design of a needle guiding mechanism. The results may find further application in training, and a better understanding and possible improvement in peripheral VP technique.

While there are many techniques and methods for enhancing or improving VP and VC success [e.g. 4–7], much of the associated modelling has been applied to needle injections into deep central tissues such as liver [8, 9], often assisted by ultrasound [10] or computed tomography [11], rather than to the peripheral VP process. De Boer *et al.* [1] have developed an instrument for automated VP and analysed the forces produced in phantom and animal tissues. However their device inserted the needle in a straight-line

path rather than the more subtle non-linear trajectory employed in actual clinical practice.

The current work focuses on the dynamics of the VP action, and is not concerned with other elements of the VP process, such as the location of a suitable injection site. This is assumed to be determined by the practitioner either by the usual sighting identification and/or sometimes with the aid of touching and feeling for the pulse or bulge of a vein. If available, some sophisticated imaging vein location technologies [2] have also been developed to aid location and identification of a suitable site. Once the injection site has been determined, the present analysis could be valuable in assisting the accurate insertion of the shaft of the venous access needle (hereafter simply referred to as “the needle”) at the predetermined site, at a predetermined or adjustable path. Section II shows how these paths, at least for a particular ideal setting, can be predetermined by realising in the model the VP process in the direct method consists of sequential steps. In section III, we consider the model in real application situations and introduce the concept of a guided VP device. In section IV, a prototype device inspired from the work in the previous sections, which can potentially aid peripheral VP, is described.

2 Physical models and methods

In particular, we consider a physical model of a peripheral VP process with four of its most important steps included, as shown in Figure 1, which is a schematic sketch of the side profile of the main components of a transfusion set, consisting of the shaft of the venous access needle 11, the body hub 13, and the corresponding tubing component 14. Note the current model assumes the injection site and vicinity is level and the vein parallel and close to the surface of skin e.g. as most commonly encountered at VP sites at the back of the hand. More complicated surface or vein geometry can be readily generalised from the basis of the current analysis.

Step 1: The VP practitioner will first identify an ideal vein and location of the injection site. Once a site is identified, the needle should enter the injection site, through the skin layer, and then into the vein at an appropriate angle. The steepness of the initial entry angle depends on how far the vein is below the surface of the skin and the size of the vein. The VP practitioner will in general decide on the steepness of entry before he/she starts the puncturing motion. The injection site should be as close as possible laterally to the middle section of the vein to minimise unne-

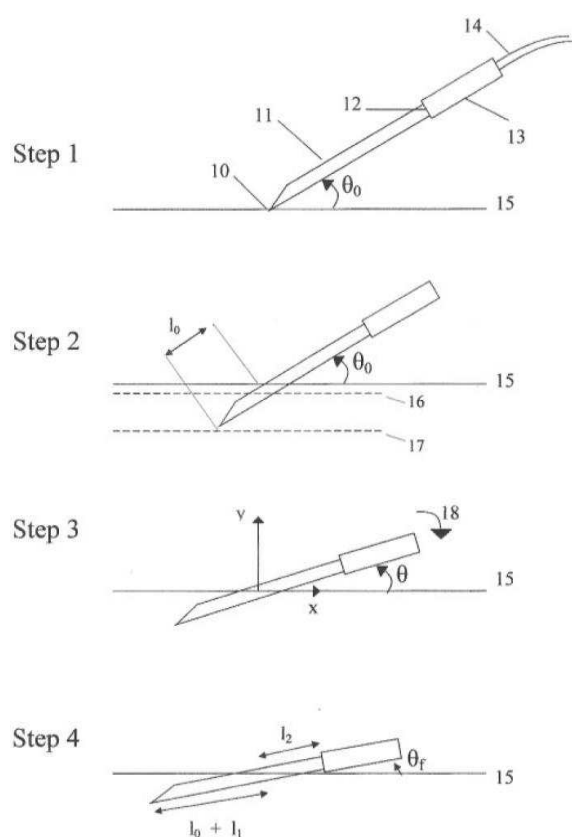


Figure 1: A side profile view of the peripheral venepuncture action.

essary venous damage and mitigate against vein or body movement. Hence, the practitioner takes aim, at desired injection site 10, with needle 11 at an initial entry angle θ_0 with respect to the injection site surface 15. The tubing component 14 of the transfusion set is omitted in the remaining parts of Figure 1 for clarity.

Step 2: The practitioner makes a sharp straight through venepuncture at fixed angle θ_0 to a desired depth. This desired depth optimally corresponds to when the tip of the needle has passed through the skin layer and subsequently safely passed through the upper side of the vein 16, but before it hits the underside of the same vein 17, the vein's side profile outline being shown as a dashed line. The length of this desired depth is represented by l_0 , as measured along the longitudinal length of the needle.

Step 3: The practitioner now inserts the needle further into the vein, accompanied by a simultaneous levelling of the needle (*i.e.* reducing the angle of penetration θ as shown by the direction arrow 18) until the needle is felt to be quite securely within the volume of the vein. A Cartesian (x, y) coordinate system is indicated with the origin (0,0) corresponding to the initial injection site 10.

Step 4: Assuming the venepuncture has been successful (as often assessed in practice from observation of blood “flashback” in the tubing of the transfusion set) the practitioner stops the venepuncture motion, possibly accompanied by minor adjustments, such that the body hub part of the transfusion set is more or less resting stably on the patient's skin to minimise tearing stress at the injection site.

The assumed final resting angle of the needle with respect to the surface of the injection site 15 of this final motion is indicated by θ_f and the total length of the needle inside the patient's tissues is $(l_0 + l_1)$, where l_1 is the additional length of the needle that has been inserted during steps 3 and 4. If l_2 represents the length of the part of the needle outside the injection site 10, then the total length L of the needle satisfies the relation $L = l_0 + l_1 + l_2$.

The above steps model the physical VP process, whereby the path and motion of the needle can potentially be predetermined. The following mathematical analysis shows a method of predicting this dynamical process.

The VP action can be systematically represented by following the motion of any particular point in the needle. Let r represent the distance from the injection site 10, to the designated top point of the needle 12 (referred to in later figures as the TN point). So, at injection site 10, $r = 0$ and this represents the origin ($r = 0$) of a polar co-ordinate system (r, θ). The motion of the VP processes described above can be analysed by following the motion of the point 12 (r, θ) relative to the injection site 10, at the origin.

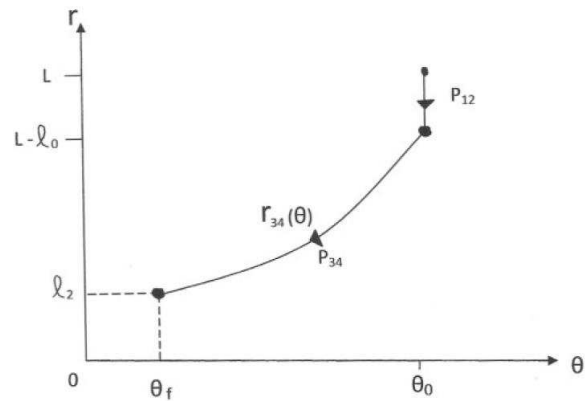


Figure 2: The dynamics of the venepuncture action, following the top of the needle (the TN-point, item 12 of Fig. 1) summarised in polar coordinates.

Figure 2 shows a plot of point 12 in the polar coordinate system (r, θ). Here P_{12} represents the path described between Step 1 and Step 2, and P_{34} is the path described in Steps 3 and 4, where $r_{34}(\theta)$ is the general equation representing this path. Note, the arrows for P_{12} and P_{34} in the figure indicate the temporal order of the dynamical VP action.

From the expected motion and constraints, $r_{34}(\theta)$ can be approximated, without losing significant accuracy or generality, as a straight line which intersects $(L - l_0, \theta_0)$ and (l_2, θ_f) . It can be readily shown that

$$r_{34}(\theta) = m\theta + r_0 \quad (1a)$$

Where,

$$m = \frac{l_1}{\theta_0 - \theta_f} \quad (1b)$$

and

$$r_0 = L - l_0 - l_1 - m\theta_f \quad (1c)$$

Since the VP process is a dynamical motion, the supposed paths can be emulated best from models which follow its time evolution. The time dependency can be introduced via the speed at which the needle is being inserted in the VP steps described. Hence, between Step 1 and Step 2, the needle can be assumed to be inserted at a particular rate $v_{12}(t)$ over the period $0 < t < t_0$, where $t = 0$ corresponds to the start of the VP process when the needle is just above the injection site 10, and about to enter the tissue, and t_0 is the time when the depth of the needle inserted has reached l_0 . The path P_{12} can in general be described by

$$r_{12}(t) = L - \int_0^t v_{12}(t) dt \quad (2a)$$

75

and

$$\theta_{12}(t) = \theta_0 \quad (2b)$$

for period $0 < t < t_0$.

The path is a straight line forming an angle $\theta = \theta_0$ with the local horizontal surface of the injection site 15 (refer to Figure 1). It is easier to visualise the path in Cartesian coordinates (x,y) where $x = r \cdot \cos(\theta)$ and $y = r \cdot \sin(\theta)$; thus, path P_{12} in Cartesian coordinates is given by

$$x_{12}(t) = r_{12}(t) \cos \theta_0 \quad (2c)$$

and

$$y_{12}(t) = r_{12}(t) \sin \theta_0 \quad (2d)$$

or

$$y_{12} = x_{12} \cdot \tan \theta_0 \quad (2e)$$

10 P_{12} is a straight line motion with the anticipated gradient $\tan(\theta_0)$.

Similarly, for path P_{34} , which occurs over the period $t_0 < t < t_f$, its equations of motion are:

$$r_{34}(t) = L - l_0 - \int_{t_0}^t v_{34}(t) dt \quad (3a)$$

and hence from Eqs. (1a, 1b, 1c)

$$\theta_{34}(t) = \frac{1}{m} [r_{34}(t) - r_0] = \frac{1}{m} \left[l_1 + m\theta_f - \int_{t_0}^t v_{34}(t) dt \right] \quad (3b)$$

15 In Cartesian coordinates,

$$x_{34}(t) = r_{34}(t) \cos \theta_{34}(t) \quad (4a)$$

and

$$y_{34}(t) = r_{34}(t) \sin \theta_{34}(t) \quad (4b)$$

which gives the coordinates (x,y) of the path P_{34} as a function of time, with the corresponding instantaneous gradient of the needle given by

$$\frac{y_{34}(t)}{x_{34}(t)} = \tan [\theta_{34}(t)] \quad (4c)$$

20 The above equations provide the generic formulae of the path and direction which the intravenous (IV) needle follows. To illustrate the above analysis in determining the path structures, it is necessary to assign the velocity profiles $v_{12}(t)$ and $v_{34}(t)$. Figure 3 shows an illustrative simplified profile model during a typical realistic VP process i.e. the needle is rapidly inserted into the injection site at an initial velocity v_0 , whereby it slows down somewhat when the tip of the needle passes the first vein wall at about $t = t_0$. After that, the velocity profile must

decrease with time (or equivalently with the depth of penetration), so that the needle motion in path P_{34} must eventually come to a halt at the desired depth of penetration of $(l_0 + l_1)$, at time $t = t_f$. This profile can be approximated by quadratic or higher polynomial functions, or numerical representations if necessary. However, it is possible to obtain revealing analytical solutions, without losing the general significance of the result, by approximating the more realistic velocity profiles of Figure 3, by a constant velocity profile approximation where $v_{12}(t) = v_0$, and a linear decreasing function $v_{34}(t)$ which satisfies the boundary conditions $v_{34} = v_0$ at $t = t_0$ and $v_{34} = 0$ at $t = t_f$. This is illustrated in Figure 4. Note that this first approximation of the velocity profile could potentially be improved upon in future versions of the model. The first part of this profile leads to the relations 45

$$v_0 = \frac{l_0}{t_0} \quad (5a)$$

and

$$\int_0^t v_{12}(t) dt = v_0 t \quad (5b)$$

and the latter profile leads to

$$v_{34}(t) = \frac{v_0}{t_f - t_0} [t_f - t] \quad (6a)$$

so that

$$\int_{t_0}^t v_{34}(t) dt = \frac{v_0}{t_f - t_0} \left\{ t_f (t - t_0) - \frac{1}{2} (t^2 - t_0^2) \right\} \quad (6b)$$

The path P_{34} can be deduced by substituting Eq. (6b) into Eqs. (3a, 3b) or Eqs. (4a, 4b).

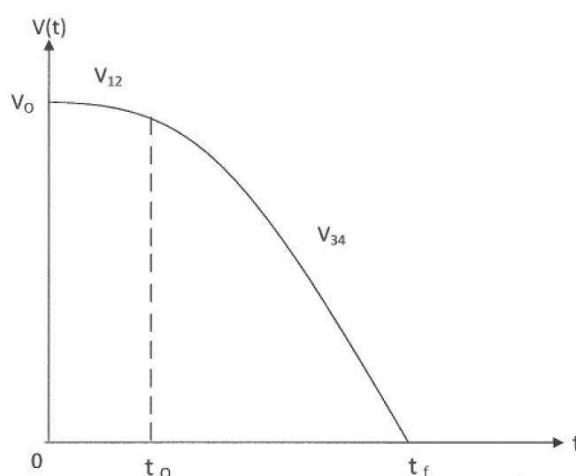


Figure 3: A typical velocity profile of the needle during the venepuncture motion, where v_0 is the initial insertion speed.

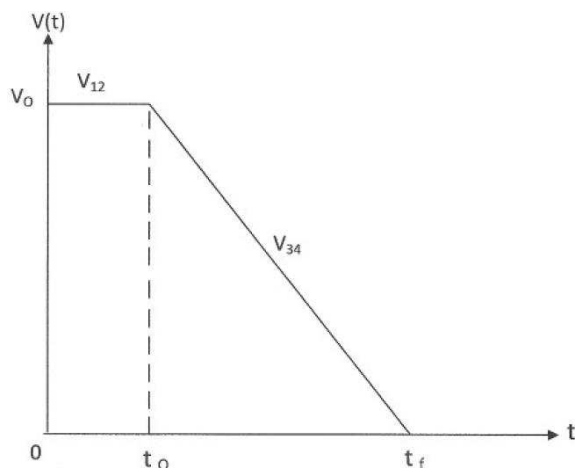


Figure 4: A first approximation to the velocity profile of Fig. 3 for modelling purposes. The proposed framework permits other approximations to be included in the future.

3 Practical applications of the model

Further insights into the VP process can be gained by plotting the path predicted by these equations using real life situations. Consider a shallow entry VP process (e.g. as most commonly associated with IV injection on the dorsum of the hand or other sites where the veins tend to be more flat and lying close to the surface). Initial injection entry and final resting angles of the needles would be shallow e.g. typically about $\theta = 10^\circ$ and $\theta = 3^\circ$ respectively. We assume the venous access needle is $L = 18$ mm and the user would typically make a sharp initial insertion of around $l_0 = 3$ mm, which would typically take a fraction of a second, e.g. $t_0 = 0.3$ sec, or equivalently an initial insertion speed of 10mm/sec. The practitioner then proceeds to Steps 3 and 4 of the VP process, allowing an element of flexibility in the rate and depth of needle movement. Assuming the injection is successful and the vein structure allows it, the user would insert a significantly longer section of the needle to the vein to increase stability.

Depending on practitioner style and habit, this would mean that l_1 could typically take a value of around $l_1 = 10$ mm. Although inexact, t_f would likely be several times larger than t_0 , with expected values of t_f of 1 to 2 sec. By varying the value of t_f in the above model, the approximate time can be determined, corresponding to the current model, when the needle has reached its final resting position of $\theta = \theta_f$, and $l_2 = L - l_0 - l_1$.

Figure 5A and 5B show respectively plots of (x,y) and its corresponding instantaneous gradient y/x (equiv-

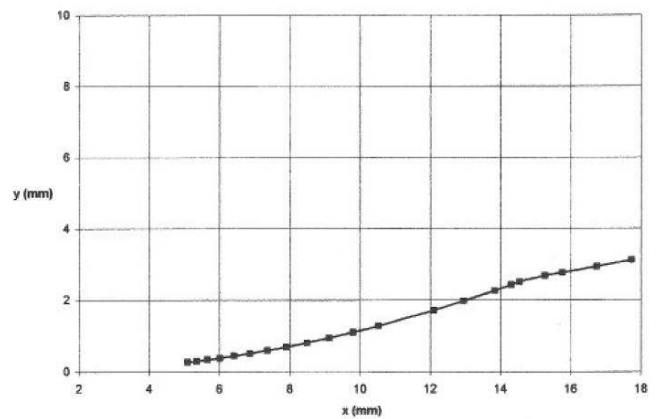


Figure 5A: The position of the needle (tracking the TN-point, equivalent to point 12 in Fig. 1) during the VP action for an initial shallow injection angle situation, where $\theta_0 = 10^\circ$ and length of the needle is 18 mm.

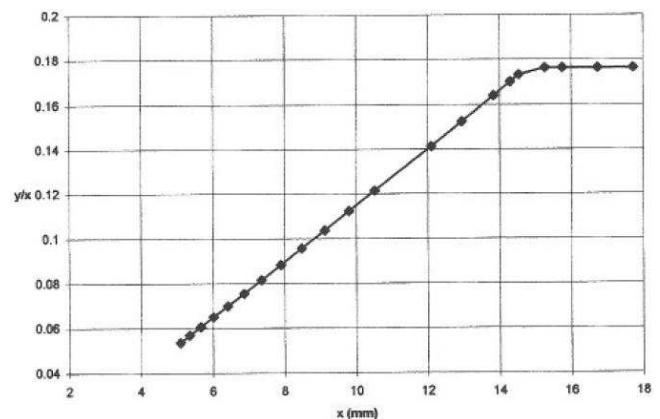


Figure 5B: The gradient of the needle during the VP action for the motion corresponding to Fig. 5A.

alently, the slope of the needle) of the point 12 (see Figure 1). Similarly, Figure 6A and 6B shows the same plots but changing the values of θ_0 only, to $\theta_0 = 30^\circ$ which corresponds to another common VP scenario, whereby the initial IV injection angle is much steeper and is most relevant for deeper lying or larger veins typically found, for instance, at the crook of the arm (i.e. the antecubital fossa).

3.1 Guiding of VP Process

The above analysis and examples show that for a particular VP situation, the desirable VP path of the needle can be usefully anticipated and therefore potentially controllable. One method of controlling the needle to follow the desirable VP path is to handle or assist the guiding of a component or part of the transfusion set which is rigidly connected with the needle, such that the TN-point follows the desired path. We shall introduce below a particular

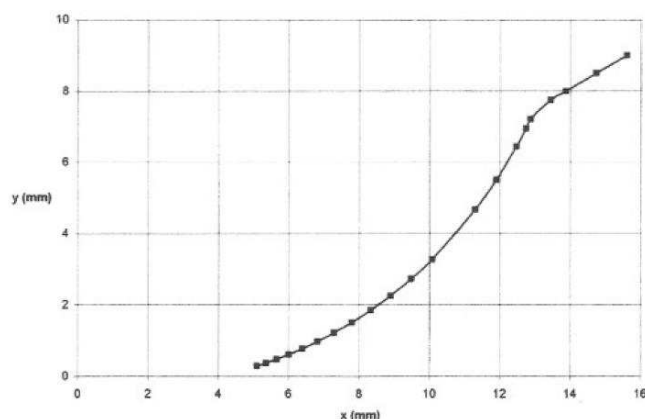


Figure 6A: The position of the needle (tracking the TN-point, equivalent to point 12 in Fig. 1) during the VP action for an initial injection angle situation, where $\theta_0 = 30^\circ$ and length of the needle is 18 mm.

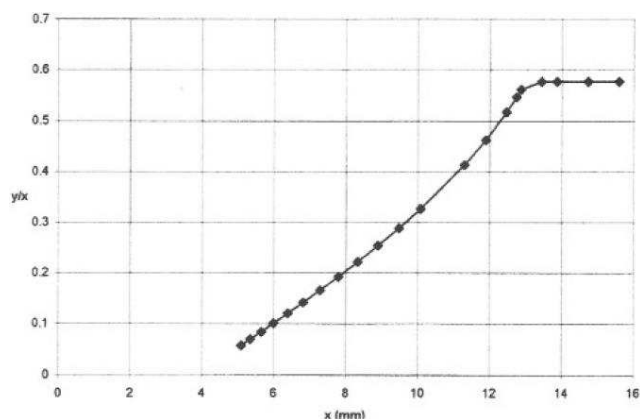


Figure 6B: The gradient of the needle during the VP action for motion corresponding to Fig. 6A.

example of a modified venous access transfusion set using this approach, in order to generalise and introduce the geometry of the analysis, with application potentials. The component can be a thin rod structure or specially adapted shaped structure extending out of the body hub of the transfusion set. This component could act as a gliding mechanism, or as a holding system for handling needle motion control, which may be located away from the body hub of the transfusion set.

Figure 7A shows a new type of winged venous access needle transfusion set (see Kam [5]), the glider assisted venous access needle set (GAv needle). The name and purpose of the glider (20) will become clear in the next section where we describe its function in a proposed IV injection aid. For illustration clarity, it is shown with the needle pointing upward and tilting slightly away from the plane of the paper. There are two new parts compared to an ordinary transfusion set, namely a large flat extended tail-wing-like part called the ‘handling wing’ (19), which

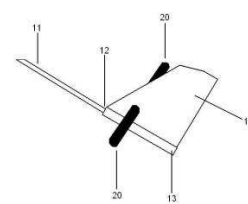


Figure 7A: A new type of peripheral venous access needle incorporating a glider component 20 for needle motion control.

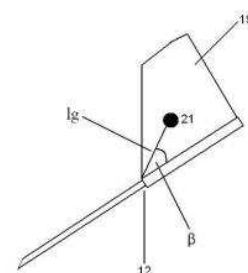


Figure 7B: A side profile of the venous access needle of Fig 7A, where the position of the glider is labelled the G-point.

is rigidly connected to the original body hub (13) of the transfusion set, and a pair of thin extended bars forming the glider, which is rigidly and symmetrically connected to each side of the handling wing.

Figure 7B shows the GAv needle set in the same side-on view in the same sense as Figure 1, where the dotted point 21 is the geometric central point of the tip of the glider and is called the glider point or G-point. An important feature of the current analysis is the control of the glider, or effectively the control of the G-point path to realise an effective VP aid. In the light of the above analysis on the motion of the TN point, it is an aim to emulate the same desirable TN point path, via the equivalent path dynamic of another point (i.e. the G-point) away from the TN point where it can be controlled or handled.

3.2 Dynamics of the transfusion set

For generality, let the length of the line joining the TN point and the G-point be indicated by l_g and the angle this line makes with respect to the body hub of the new gliding transfusion set be indicated by β , as illustrated in Figure 7B. By denoting the location of the G-point 21 by (X, Y) , it can be readily shown that for TN point with coordinates (x, y) , that

$$X(t) = x(t) + l_g \cos(\theta(t) + \beta) \quad (7a)$$

$$Y(t) = y(t) + l_g \sin(\theta(t) + \beta) \quad (7b)$$

Note that for $\beta = 0$, the gradient of the line joining the injection site (point 10 in Fig. 1), and the G-point is the same as the gradient of the needle *i.e.* $Y(t)/X(t) = y(t)/x(t)$.

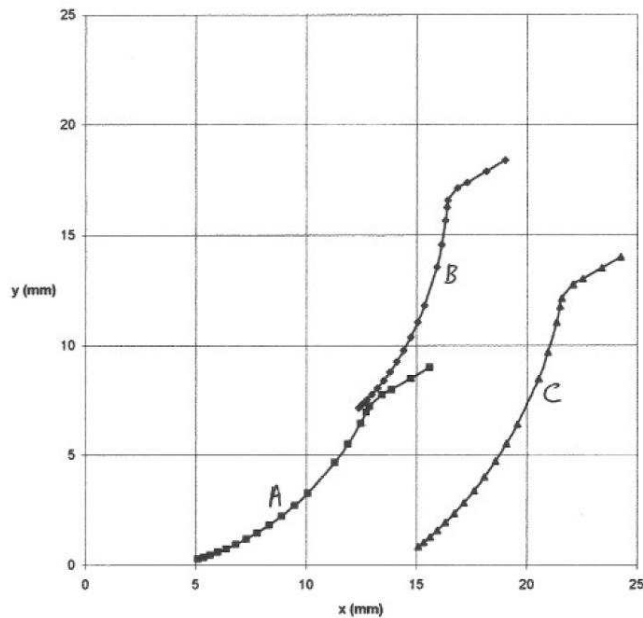


Figure 8A: Showing the trajectories of the transfusion set for the TN-point (curve A), the paths of the G-points with $l_g = 10$ mm, $\beta = 40^\circ$ (curve B) and $l_g = 10$ mm, $\beta = 0^\circ$ (curve C). All other parameters same as for Figure 6A.

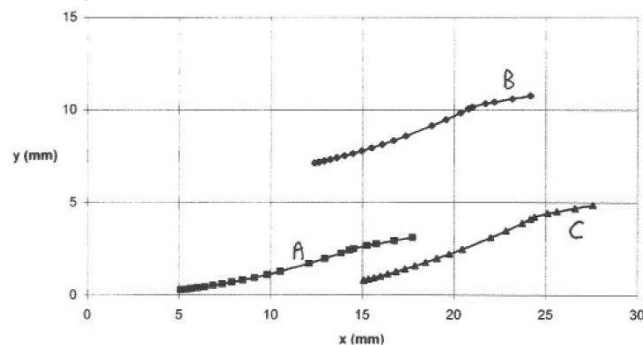


Figure 8B: Showing the trajectories of the transfusion set for the TN-point (curve A), the paths of the G-points with $l_g = 10$ mm, $\beta = 40^\circ$ (curve B) and $l_g = 10$ mm, $\beta = 0^\circ$ (curve C). All other parameters same as for Figure 5A.

point (and so the glider) allows a flexible or optimal design solution for any VP aid that may rely on the principle of controlling the path and gradient of the needle via a mechanical control and constraints placed on the movement of the glider. The G-point location for the curve B case approximates the common related position where a VP practitioner would be controlling the needle by the folded wing of a conventional butterfly® wing transfusion set. Thus curve B illustrates best the path taken by the holding fingers of the VP practitioner when administering this particular VP action.

For comparison, Figure 8B shows the paths of the TN point (curve A) and the two possible paths of the G-point 21 (X,Y) with $l_g = 10$ mm, $\beta = 40^\circ$ (curve B) and $l_g = 10$ mm, $\beta = 0^\circ$ (curve C), the difference from Figure 8A being that the other parameters are the same as those for Figure 5A (*i.e.* $\theta_0 = 10^\circ$).

4 A peripheral IV injection aid

4.1 The device

Being able to calculate a VP trajectory for a particular initial condition means we could potentially design a device to emulate or facilitate such action. In this section we show a peripheral IV injection aid which was inspired by the above work. This device comprises two parts: 1) a modified butterfly® type needle, similar to the GAv needle set as mentioned above, and 2) a specially designed guide, hereafter referred as the S-guider, which works with the GAv needle to assist in the VP action.

Figures 9 & 10 show respectively a functioning prototype of a S-guider and its corresponding GAv needle, with needle length $L=18$ mm. The glider components in this GAv needle is effectively allocated at the TN point *i.e.* the G-

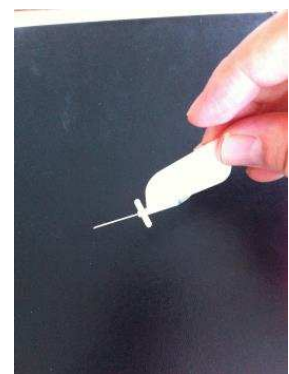


Figure 9 & 10: The S-guider & The GAv needle set.

Using the same set of parameters as Figure 6A (*i.e.* $\theta_0 = 30^\circ$), Figure 8A shows the paths of the TN point (curve A) and the two possible paths of the G-points (X,Y) with $l_g = 10$ mm, $\beta = 40^\circ$ (curve B) and $l_g = 10$ mm, $\beta = 0^\circ$ (curve C). This figure shows that the positioning of the G-

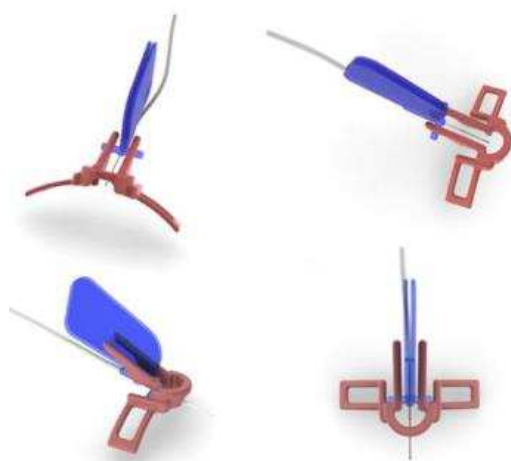


Figure 11: CAD illustrations of the peripheral intravenous injection aid.

point is specified at $l_g = 0$, and $\beta = 0$. This GAv needle set has an elongated handling wing to enable the VP practitioner to handle it a bit further away from the G-point, because the VP procedure is performed in conjunction with the S-guider which have protruding features which would otherwise interfere with the practitioner's fingers.

Assuming a peripheral injection site is identified, the S-guider is placed over it, with the injection site approximately in the geometric centre of the quasi semi circular open area. The whole S-guide can then be securely anchored to the patient via the extended wing like structure being taped down.

The guider arms shown in this prototype are fixed at 30 degrees relative to the base frame. Hence its underside has a profile consisting of a straight edge and a curved edge, similar to that shown in Fig. 6A, which when connected to glider of GAv needle will assist in guiding the needle into the vein. The straight edge provides the initially sharp insertion of the needle into the vein, and the curve edge initiates and forces a gentle levelling of the needle into it (*i.e.* step 3 of Figure 1).

4.2 Experiments

The S-guider discussed was made using the SLA rapid prototype technique.. Although relatively fragile compared to a properly made device using a more flexible material, we were able to test the functionality of the device, by practicing VP actions on a VP training pad made of latex free Dermalike™ skin with artificial veins. This crude prototype performed remarkably well, providing a consistent performance of enabling the needle to repeatedly slide

into a peripheral vein without over puncture. Note that we subsequently carried out most of the further testing on a mandarin fruit, which provides a surprisingly realistic feel compared to the over tough skins found on the VP training kit. Before the device was made, we were concerned about the feel of using it and applicability in varying realistic VP conditions, and in particular confirmed the following three points: a) the sliding of the glider against the guider arms during the VP process did not present a noticeable or objectionable contact resistance; b) the need to hold an elongated handling wing did not present any extra difficulties, c) although the profile and angles of the guider arms were based on a 30 deg initial injection setting, we found the same device could be applied quite flexibly over much wider initial injection angle situations. For example, when one wishes to initiate a deeper initial needle entry, the device can accommodate this since, in most injection sites, the skin on which the base of the S-guider is attached have some flexibility of movement. Conversely, a VP situation which requires a less steep initial entry could still make use of the device; the straight part of the guider arms are simply not used, whilst the curved part of the guider arms could still help to prevent over puncture action. In conclusion, the device has demonstrated the principle that VP action can be effectively guided, with the potential to enhance or assist in some peripheral intravenous injection situations. The work needs to be validated further with clinically approved models, and with clinical trials conducted on animal or human subjects. Figure 11 shows CAD drawings of the prototype in clearer detail.

4.3 Data Collection

We made additional experimental observations by recording a series of videos of the VP process carried out by an experienced VP practitioner. A VP training pad was used made of latex free Dermalike™ skin with artificial veins. Custom software was written allowing for a frame-by-frame analysis of the videos (Figure 12), in which multiple points on the needle shaft 11 were tracked. Data was averaged and normalised across multiple videos leading to a final data point set. From these points, a needle vector was created, and injection angle (Figure 13) and velocity profiles (Figure 14) were generated from this vector data and related to the model.

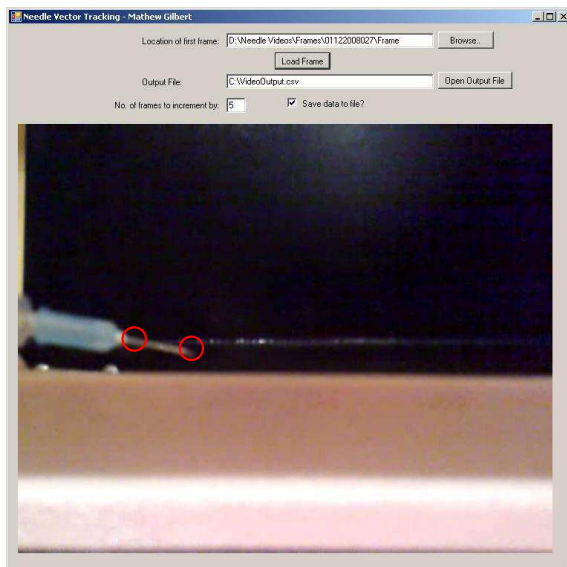


Figure 12: Needle vector tracking software for tracking the motion of the needle during VP. The points circled (red) were used for the velocity and angle profiles shown in Figures 13 and 14.

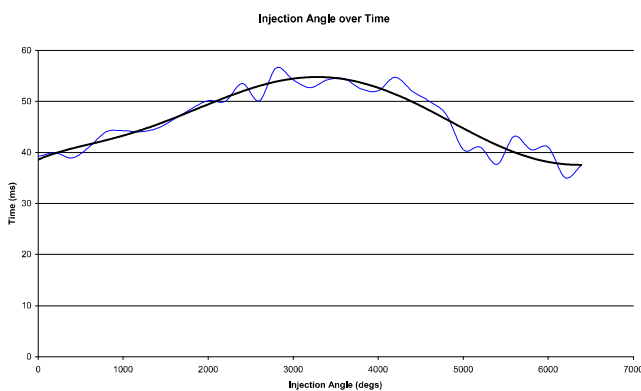


Figure 13: Variance in needle vector angle during VP process from a video recording of a typical peripheral venepuncture application.

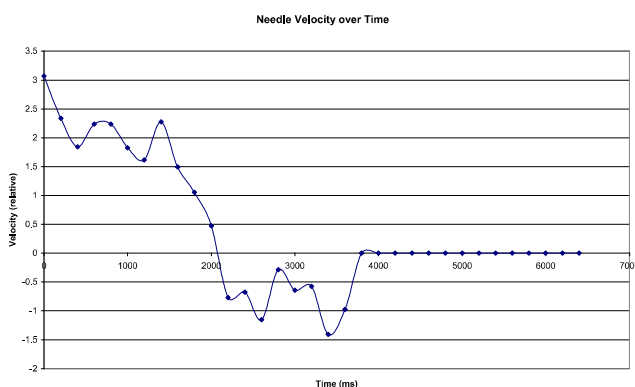


Figure 14: Needle vector velocity during VP process derived from a video recording of a typical venepuncture application.

5 Conclusions

An instructive mathematical model for analysing and controlling the VP action and its needle trajectories has been formulated for the direct method. The analysis involves two distinct sets of parameters. The first set of parameters are those specific to the nature of the VP process associated with human interaction and decision, corresponding to the initial angle of injection θ_0 , the length of the initial linear entry of the needle shaft l_0 , subsequent further length of the needle shaft l_1 , which enters into the vein via a curvilinear motion, the velocity profile of the VP action (i.e. as specified by V_{12} and V_{34} of Figure 3) and the desired final resting angle of the needle shaft θ_f . The second set are those parameters specific to the design of the VP transfusion set, corresponding to the length of the needle shaft L , and the position of the control pivot point, i.e. the glider point, or G-point, as specified by l_g and β . The analysis can also be used to define how the orientation and movement of the venous access needle is best controlled via appropriate handling and constraints applied to the rigid body part of a proposed transfusion set (i.e. control of the G-point path to achieve the desirable calculated VP path). The analysis sets out design equations which can be used with relevant parameters to achieve accurate predictions of the G-point path, and thus also enable optimal design and control of any needle, via control on the G-point movement. These equations describe non-linear dynamical paths of the needle as may occur in a clinical application, that may assist in the automation of the VP process e.g. by robotic control or some guiding mechanism. For illustration, we have created and demonstrated a medical device designed using our model, the S-guider and GAV needle set combination, with potential to assist in peripheral intravenous injection.

The model is based on a simple geometric approach, combined with dynamical consideration of needle velocity profiles, and does not take account of needle force dynamics nor interactions with any material properties of the injection site. The analysis of real time VP videos indicates a number of similarities, but also differences, between the model assumptions and averaged injection profiles on a training pad. Figure 13 shows the injection time-angle profile, derived from a typical injection video, starting with an increasing needle angle prior to the needle meeting the injection point, and followed by a decrease in angle during entry into the “vein”, as indeed modelled in our analysis. In Figure 14, initial needle velocity profiles decline in a similar manner to that modelled (see Figures 3 and 4) but, unlike the model, profiles become negative prior to the

completion of the VP process. Observation of the videos shows that this is the result of a push-back on the needle from the training pad (made of a resilient rubber-like material) as the practitioner releases their hold slightly when injecting the notional substance. Additional work is required to determine whether a negative velocity profile also takes place in injections conducted *in vivo*. However, as this push back occurs at the conclusion of the injection process, its presence if confirmed would not compromise the validity or application of the reported approach.

Our model is based on a simplified direct method of application and is not intended to capture all aspects and techniques associated with the full range and variety of VP procedures. We anticipate that our results could be particularly useful in providing a framework for future modelling and development of an automated venepuncture machine, particularly if combined with the approach and experimental techniques involving force parameters and insertion force feedback, as studied for example by De Boer *et al.* [1] and Okamura *et al.* [9].

In summary, the present work demonstrates a method whereby the VP action can be readily modelled, enabling a better understanding and visualisation of the dynamic of the VP action, with potential as a teaching aid and applications in assistive medical technology.

Acknowledgement: KFK gratefully acknowledges grant support from BusinessLink Yorkshire for the development of the injection aid prototypes, which was made by the Design Department of Sheffield Hallam University led by principal designer Anthony Jones. KFK also acknowledges useful discussion of the VP process with Angela Westoby, Haemophilia Nurse Specialist, at St James's Hospital, Leeds, UK. The experimental videos used for analysis were recordings of injections undertaken for this study by Dr Fiona C. Pelah.

References

- [1] Boer T. De, Steinbuch M., Neerken S., Kharin A., Laboratory study on needle-tissue interaction: towards the development of an instrument for automatic venepuncture. *Journal of Mechanics in Medicine and Biology* 2007, 7, 325–335 40
- [2] Miyake R.K., Zeman H.D., Durate F.H., Kikuchi R., Rammacciotti E., Lovhoiden G., Vrancken C., Vein Imaging: A new method of near infrared imaging, where a processed image is projected onto the skin for the enhancement of vein treatment. *Dermatologic Surgery* 2006, 32:8, 1031–1038 45
- [3] Mbamalu D., Banerjee A., Classic techniques in medicine: Methods of obtaining peripheral venous access in difficult situations. *Postgrad. Med. J.* 1999, 75, 459–462
- [4] Lenhardt R., Seybold T., Kimberger O., Stoiser B., Sessler D.I., 2002, Local warming and insertion of peripheral venous cannulas: single blinded prospective randomized controlled trial and single blinded randomized crossover trial. *BMJ*;325:409;12 50
- [5] Kam K.F., Intravenous injection aid. International patent application no.: PCT/GB2008/003425. Published 11 June 2009 under WO2009/047512 55
- [6] Roberge R.J., Venodilatation techniques to enhance venepuncture and intravenous cannulation. *The Journal of Emergency Medicine* 2004, 27, No.1, 69–73
- [7] Samantaray A., Intravenous access: A different approach. *J. Indian Assoc. Pediatr Surg* 2007, 12 Issue 3, 163 60
- [8] DiMaio S.P., Salcudean S.E., Needle steering and motion planning in soft tissues. *IEEE Trans. Bio-Med. Eng.* 2005, Vol 52, pp. 965–974
- [9] Okamura A.M., Simone C., O'Leary, M.D., Force modeling for needle insertion into soft tissue. *IEEE Trans. Bio-Med. Eng.* 2004, Vol 51, pp. 1707–1716 65
- [10] Calvert N., Hind D., McWilliams R.G., Thomas S.M., Beverley C., Davidson A., The effectiveness and cost-effectiveness of ultrasound locating devices for central venous access: a systematic review and economic evaluation. *Health Technology Assessment* 2003, Vol. 7, No 12 70
- [11] Vidal F.P., Chalmers N., Gould D.A., Healey A.E., John N. W., Developing a needle guidance virtual environment with patient-specific data and force feedback. *International Congress Series* 2005, 1281, pp. 418–423 75
- [12] Ingram P., Lavery I., Peripheral intravenous cannulation: safe insertion and removal technique. *Nursing Standard.* 2007, 22, 1, 44–48.